

Boundary layer emission in luminous LMXBs

M.GILFANOV^{1,2} and M.REVNIVTSEV^{1,2}

¹ Max-Planck-Institute für Astrophysik, Karl-Schwarzschild-Str. 1, D-85740 Garching bei München, Germany,

² Space Research Institute, Russian Academy of Sciences, Profsoyuznaya 84/32, 117997 Moscow, Russia

Abstract. We show that aperiodic and quasiperiodic variability of bright LMXBs – atoll and Z- sources, on \sim sec – msec time scales is caused primarily by variations of the luminosity of the boundary layer. The emission of the accretion disk is less variable on these time scales and its power density spectrum follows $P_{\text{disk}}(f) \propto f^{-1}$ law, contributing to observed flux variation at low frequencies and low energies only. The kHz QPOs have the same origin as variability at lower frequencies, i.e. independent of the nature of the “clock”, the actual luminosity modulation takes place on the neutron star surface. The boundary layer spectrum remains nearly constant in the course of the luminosity variations and is represented to certain accuracy by the Fourier frequency resolved spectrum. In the investigated range of $\dot{M} \sim (0.1 - 1)\dot{M}_{\text{Edd}}$ it depends weakly on the global mass accretion rate and in the limit $\dot{M} \sim \dot{M}_{\text{Edd}}$ is close to Wien spectrum with $kT \sim 2.4$ keV. Its independence on the global value of \dot{M} lends support to the theoretical suggestion by Inogamov & Sunyaev (1999) that the boundary layer is radiation pressure supported.

Based on the knowledge of the boundary layer spectrum we attempt to relate the motion along the Z-track to changes of physically meaningful parameters. Our results suggest that the contribution of the boundary layer to the observed emission decreases along the Z-track from conventional $\sim 50\%$ on the horizontal branch to a rather small number on the normal branch. This decrease can be caused, for example, by obscuration of the boundary layer by the geometrically thickened accretion disk at $\dot{M} \sim \dot{M}_{\text{Edd}}$. Alternatively, this can indicate significant change of the structure of the accretion flow at $\dot{M} \sim \dot{M}_{\text{Edd}}$ and disappearance of the boundary layer as a distinct region of the significant energy release associated with the neutron star surface.

Key words: accretion, accretion disks – instabilities – stars:binaries:general – stars:neutron – X-rays:general – X-rays:binaries

©0000 WILEY-VCH Verlag GmbH & Co. KGaA, Weinheim

1. Introduction

Accreting neutron stars in low mass X-ray binaries (LMXB) are among the most luminous compact X-ray sources in the Milky Way. A number of them have luminosities exceeding $\sim \text{few} \times 10^{38}$ erg/s and presumably accrete matter at the level close to the critical Eddington accretion rate. In the bright state these sources have rather soft X-ray spectra, indicating that their X-ray emission is predominantly formed in the optically thick media. Similar to black holes, at lower luminosities, $\log(L_X) \lesssim 36.5 - 37$, neutron stars undergo a transition to the hard spectral state (e.g. Barret, 2001). The energy spectra in this state point at the low optical depth in the emission region, indicating a significant change of the geometry of the accretion flow.

In the soft spectral state, the commonly accepted picture of accretion at not too extreme values of accretion rate has two main ingredients – the accretion disk (AD) and the boundary layer (BL). While in the disk matter rotates with

nearly Keplerian velocities, in the boundary layer it decelerates down to the spin frequency of the neutron star and settles onto its surface. For the typical neutron star spin frequency ($\lesssim 500 - 700$ Hz) comparable amounts of energy are released in these two regions (Sunyaev & Shakura, 1986; Sibgatullin & Sunyaev, 2000). This picture is based on rather obvious qualitative expectations as well as more sophisticated theoretical considerations and numerical modeling (Sunyaev & Shakura, 1986; Kluzniak, 1988; Inogamov & Sunyaev, 1999; Sibgatullin & Sunyaev, 2000). It has been receiving, however, little direct observational confirmation. Due to similarity of the spectra of the accretion disk and boundary layer the total spectrum has a smooth curved shape, which is difficult to decompose into separate spectral components (Mitsuda et al., 1984; White et al., 1988; Di Salvo et al., 2001; Done et al., 2002). This made application of physically motivated spectral models to the description of observed spectra of luminous neutron stars difficult, in spite of very significant increase in the sensitivity

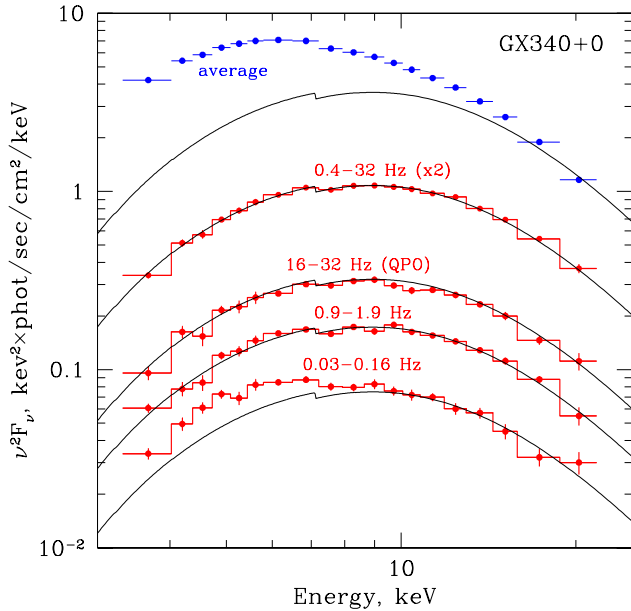


Fig. 1. Average and frequency resolved spectra of GX340+0 on the horizontal branch of the color-color diagram. The solid lines show the Comptonization spectrum with parameters similar to those given in the Section 4.

of X-ray instruments. Not surprisingly, the best fit parameters derived from the data of different instruments and, correspondingly, the inferred values of the physically meaningful quantities are often in contradiction to each other.

This ambiguity can be resolved if the spectral information is analysed together with timing data. Early results of Mitsuda et al. (1984) and Mitsuda & Tanaka (1986) suggested that the boundary layer and accretion disk may have different patterns of spectral variability. Based on the TENMA data, they studied the difference between the spectra averaged at different intensity levels – that restricted the range of accessible time scales to $\gtrsim 10^3$ sec. Gilfanov, Revnivtsev & Molkov (2003) and Revnivtsev & Gilfanov (2005) have exploited the technique of Fourier frequency resolved spectroscopy (Revnivtsev et al., 1999) to study spectral variability of luminous LMXBs in a broad range of time scales, including kHz QPO. Their findings are reviewed and discussed below.

2. Fourier-frequency resolved spectroscopy of luminous LMXBs

2.1. The method

As defined in Revnivtsev et al. (1999), the Fourier frequency resolved spectrum is the energy dependent rms amplitude in a selected frequency range, expressed in absolute (as opposite to fractional) units. A similar approach was used by Mendez et al. (1997) to study the energy spectrum of kHz oscillations in 4U0614+09. One of its advantages over fractional rms-vs.-energy dependence is the possibility to use

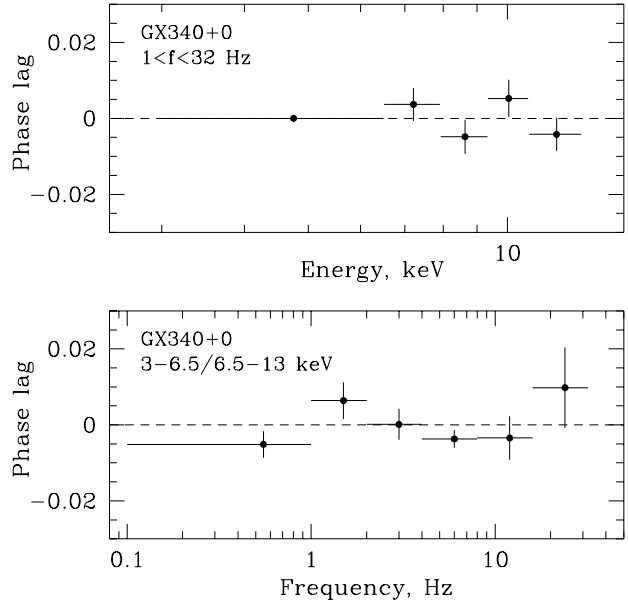


Fig. 2. Phase lags in GX340+0 on the horizontal branch as function of energy (*upper panel*) and Fourier frequency (*lower panel*). The energy dependent phase lags were computed in the 1–32 Hz frequency range, the frequency dependent lags are between 3–6.5 keV and 6.5–13 keV energy bands. The phase is normalized to 0–1 interval.

conventional (i.e. response folded) spectral approximations in order to describe the energy dependence of aperiodic variability. Although the interpretation of the frequency resolved spectra is not always straightforward, several applications of this technique to variability of black hole binaries gave meaningful results (e.g. Revnivtsev et al., 1999; Gilfanov et al., 2000).

We will use the following example as an illustration. Let us consider a two-component spectrum, consisting of a constant and variable component. The variable component changes its normalization but not the spectral shape. In this case the shape of the frequency resolved spectrum would not depend on the Fourier frequency and would be identical to the spectrum of the variable component. Importantly, the X-ray flux in all energy channels will vary coherently and with zero time/phase lag between different energies. Presence of significant phase lag and/or Fourier frequency dependence of the frequency resolved spectra would indicate that a more complex pattern of spectral variability is taking place.

With few exceptions (Dieters et al., 2000), phase lag between light curves in different energy bands in luminous LMXBs is usually small, $\Delta\phi \lesssim \text{few} \times 10^{-2}$, coherence is consistent with unity, (e.g. Vaughan et al., 1994, 1999; Dieters et al., 2000) and the behavior of the fractional rms-vs-energy dependence is similar at different frequencies (van der Klis, 1986, 2000). This suggests, that Fourier frequency resolved spectra can be interpreted in a straightforward and model-independent manner.

2.2. Results

For the case study we use archival data of PCA observations of a Z-source GX340-0 on the horizontal branch of the color-color diagram. Gilfanov, Revnitsev & Molkov (2003) conducted similar study of an atoll source 4U1608-52 and arrived at similar conclusions. Our choice was defined by the requirement that the PCA configuration combined sufficient energy resolution (large number of the energy channels) with good timing resolution and large total exposure time. The Fourier frequency resolved spectra in several frequency bands corresponding to the band limited continuum noise component and the ~ 25 Hz QPO are shown in Fig. 1 along with the conventional spectrum of the source averaged over the same data. The figure clearly demonstrates that shape of the spectra depends on the Fourier frequency at low frequencies and becomes independent of the frequency at $f \gtrsim 0.5$ Hz. Another conclusion from the data presented in Fig. 1, important for the following discussion, is that all frequency resolved spectra are significantly harder than the average source spectrum.

The phase lags as function of energy and Fourier frequency are shown in Fig. 2. No statistically significant phase lags were detected with an upper limit of $\Delta\phi \sim 10^{-2}$, where phase ϕ is normalized to the interval 0–1 (as opposed to $0 - 2\pi$).

2.3. Interpretation

We show below that independence of the frequency resolved spectra on the Fourier frequency and the smallness of the phase lags require a particularly simple form of the spectral variability.

The constancy of the spectral shape with Fourier frequency implies that the power spectrum $P(E, \omega)$ can be represented as a product of two functions, one of which depends on the energy and the other on the frequency only. For convenience we write $P(E, \omega)$ in the form:

$$P(E, \omega) = S^2(E) \times f^2(\omega) \quad (1)$$

where non-negative functions $S(E)$ and $f(\omega)$ can be directly determined from the frequency resolved spectra. The Fourier image of the light curve $F(E, t)$ is:

$$\hat{F}(E, \omega) = S(E) \times f(\omega) \times e^{i\phi(E, \omega)} \quad (2)$$

In the general case the complex argument $\phi(E, \omega)$ can depend both on Fourier frequency ω and energy E . If the phase lags between different energies are negligibly small, ϕ depends on the Fourier frequency only and the Fourier image of $F(E, t)$ is:

$$\hat{F}(E, \omega) = S(E) \times f(\omega) \times e^{i\phi(\omega)} \quad (3)$$

The light curve $F(E, t)$ can be computed via inverse Fourier transform of $\hat{F}(E, \omega)$:

$$\begin{aligned} F(E, t) &= \int d\omega \hat{F}(E, \omega) e^{i\omega t} = \\ &= S(E) \times \int d\omega f(\omega) e^{i\phi(\omega)} e^{i\omega t} = \\ &= S(E) \times f(t) \end{aligned} \quad (4)$$

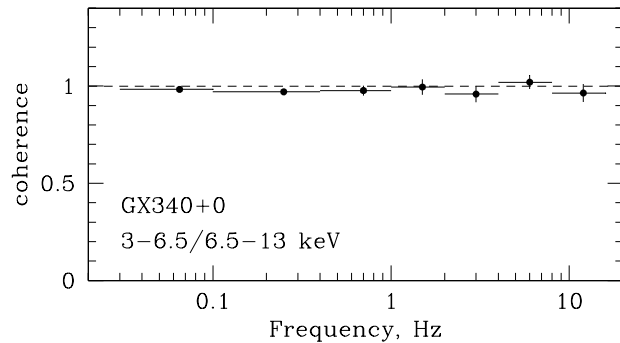


Fig. 3. GX340+0: Coherence between the light curves in the 3–6.5 and 6.5–13 keV energy bands as function of frequency. No correction for the dead time effects has been made.

An arbitrary function of energy can obviously be added to the above expression:

$$F(E, t) = S_0(E) + f(t) \times S(E) \quad (5)$$

Thus, the light curves at different energies are related by a linear transformation.

From Eq. (5) it follows that the coherence of the signals in any two energy bands is exactly unity, as they are related by a linear transformation. This prediction is in a good agreement with observations (Fig. 3).

3. Boundary layer and accretion disk emission

As follows from eq.(5), two components can be distinguished in the GX340-0 emission. The term $S_0(E)$ in Eq. (5) is the constant (non-variable) part of the source emission spectrum and $f(t)$ represents flux variations of the second, variable component.¹ The spectrum $S(E)$ of the variable component does not change in the course of flux variations and equals the frequency resolved spectrum, i.e. can be directly determined from observations.

There are two major components of accretion onto a slowly rotating weakly magnetized neutron star – (i) the Keplerian accretion disk and (ii) the boundary or spreading layer near the surface of the neutron star, in which the accreting matter decelerates to the spin frequency of the star and spreads over its surface (Sunyaev & Shakura, 1986; Kluzniak, 1988; Inogamov & Sunyaev, 1999; Popham & Sunyaev, 2001). These two geometrically distinct regions give comparable contributions to the observed X-ray emission (Sibgatullin & Sunyaev, 2000). Recalling eq.(5), it is plausible to assume, that the variable part of the X-ray emission is associated with one of these components. In order to check this assumption and to identify the variable component we consider below theoretical expectations for the disk and

¹ The possibility of small variations of the spectral parameter (e.g. temperature, optical depth etc.) is discussed by Gilfanov, Revnitsev & Molkov (2003) and is shown to be inconsistent with observations.

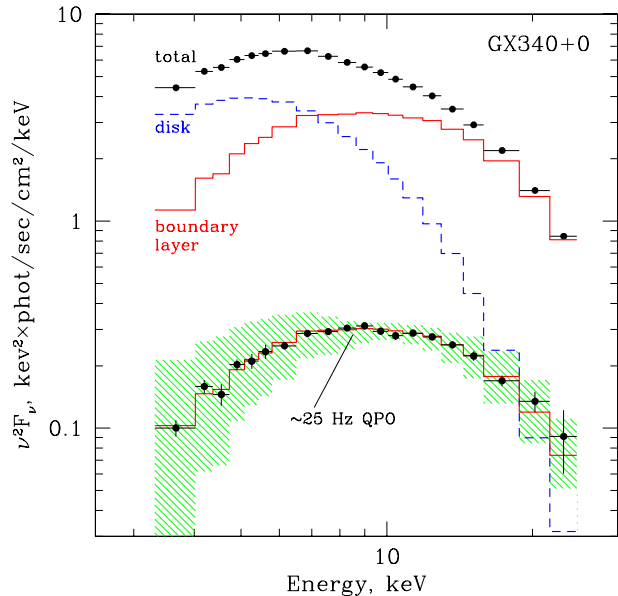


Fig. 4. The average and frequency resolved spectra of GX340+0 (horizontal branch). The shaded area shows the plausible range of the boundary layer spectra calculated as described in the section 3. The dashed (blue) histogram shows the best fit accretion disk spectrum (Gilfanov, Revnitsev & Molkov, 2003). The upper solid (red) histogram shows the boundary layer spectrum computed as the difference between the (observed) total and (predicted) accretion disk spectrum. The lower solid histogram is the same but scaled to the total energy flux of the frequency resolved spectrum.

boundary layer spectra and compare them with the observed frequency resolved spectra.

At sufficiently high values of \dot{M} both BL and disk are optically thick, as confirmed by the softness of the LMXB spectra. Simple arguments, taking into account the difference in the emitting areas suggest that the spectrum of the boundary layer should be harder than that of the accretion disk (e.g. Mitsuda et al., 1984; Grebenev & Sunyaev, 2002). Due to complexity of the boundary/spreading layer problem the theory has not advanced significantly beyond this qualitative statement – no models capable to directly predict its spectrum exist yet. Significantly better progress has been achieved in modeling spectra of accretion disks (Shakura & Sunyaev, 1973; Shimura & Takahara, 1995; Ross & Fabian, 1996). Relatively simple models of multicolor disk type which account for the effects of Compton scattering with a simple color-to-effective temperature ratio turned out to be successful in describing the accretion disk spectra observed in the high state of black hole systems (e.g. Ebisawa et al., 1991; Gierlinski et al., 1997).

For this reason we chose to use a model of the disk emission as the starting point. The BL spectrum is computed as a difference between the (observed) total spectrum and the (predicted) disk spectrum. To estimate the plausible range of the BL spectra we investigate the parameter space of the ac-

cretion disk model. For the latter we adopt the general relativistic accretion disk model by Ebisawa et al. (1991) (the “grad model” in XSPEC). The parameters of the model are: the source distance D , mass of the central object M_{NS} , disk inclination angle i , the mass accretion rate \dot{M} and the color-to-effective temperature ratio $f = T_{\text{col}}/T_{\text{eff}}$. With this approach we can predict the disk and the boundary layer spectra based on the observed X-ray flux and spectrum and very generic system parameters, such as neutron star spin frequency, the source distance etc. The procedure is described in detail in Gilfanov, Revnitsev & Molkov (2003). The obtained range of the BL spectra is shown in Fig. 4 as the shaded area. The similarity of the predicted BL spectrum and of the observed frequency resolved spectrum is obvious. On the other hand the disk spectrum is significantly softer and is inconsistent with the frequency resolved spectrum.

Gilfanov, Revnitsev & Molkov (2003) conducted similar investigation of an atoll source 4U1608-52 having ~ 10 times lower luminosity. They considered frequency resolved spectra at different frequencies, including the kHz QPOs and showed that it demonstrates behavior identical to GX340-0.

Based on these results we conclude that the X-ray variability on \sim second – millisecond time scales is related to variations of the luminosity of the boundary layer. The shape of its spectrum remains nearly constant in the course of these variations and equals the frequency resolved spectrum, i.e. can be directly obtained from the observations. This can be used to separate the boundary layer and the accretion disk contribution to the total spectrum and permits to check quantitatively the predictions the accretion disk and boundary layer models. It also opens the possibility to measure relative contributions of these two components of the accretion flow to the total observed X-ray emission.

4. Boundary layer spectrum

Based on the assumption that the frequency resolved spectra in luminous LMXBs adequately represent the boundary layer spectrum, we compare several LMXBs – atoll sources 4U1608-52 and 4U1820-30 and Z-sources Cyg X-2 and GX 17+2. Their frequency resolved spectra at frequencies $f \gtrsim$ few Hz are shown in Fig.5. As before, for Z sources we used only data on the horizontal branch of the color-color diagram, where the amplitude of variability at these frequencies is maximal. To facilitate comparison, the normalizations of all spectra were adjusted to match that of GX340+0. Similarity of the spectra is remarkable, especially considering significant difference in the average spectra and a factor of $\sim 10 - 20$ spread in the luminosity between atoll and Z-sources ($\sim 0.1\dot{M}_{\text{Edd}}$ and $\sim \dot{M}_{\text{Edd}}$ correspondingly).

The independence of the spectrum of the boundary layer on the luminosity lends support to the theoretical predictions by Inogamov & Sunyaev (1999) that the boundary layer is radiation pressure supported, i.e. radiates at the local Eddington flux limit. In this model the luminosity of the spreading layer on the surface of the neutron star changes due to variations of its area, rather than surface emissivity of the unit area. If this picture is correct, the parameters of the BL emission can

be used to determine the value of the Eddington flux limit on the surface of the neutron star. As the Eddington flux limit is uniquely determined by the neutron star surface gravity and the atmospheric chemical composition, the neutron star mass and radius can be constrained (Revnitvsev & Gilfanov, 2005).

The similarity of the spectral shape of the BL spectrum in different sources (Fig.5) indicates that there is no significant spread in the values of the mass and radius among LMXBs, in particular, that the surface gravity in atoll and Z-sources is similar. It also shows that there are no significant differences caused by variations in the atmospheric chemical abundances between sources. In particular we did not find statistically significant difference between ultra-compact compact binary 4U1820-30 and other sources.

The shape of the frequency resolved (\approx boundary layer) spectrum can be adequately described by the saturated Comptonization. For the sake of comparison with other results and for convenient parameterization of the BL spectrum we used the Comptonization model of Titarchuk (1994). The best fit parameters of the model fitted in the 3-20 keV range simultaneously to all five spectra shown in the Fig.5 are: temperature of seed photons $kT_s = 1.5 \pm 0.1$, temperature of electrons $kT_e = 3.3 \pm 0.4$ and the optical depth $\tau = 5 \pm 1$ for slab geometry. The best fit model is shown by the thick dotted line on Fig.5. The temperature of the black body spectrum describing the shape of the cutoff in the observed spectrum at energies >13 keV is $kT_{bb} = 2.4 \pm 0.1$ keV (thin dashed line on Fig.5).

The fact that kHz QPO show the same behavior as other components of the aperiodic variability indicates, that they have the same origin, i.e. are caused by the variations of the luminosity of the boundary layer. Although the kHz “clock” can be in the disk or due to it’s interaction with the neutron star, the actual modulation of the X-ray flux occurs on the neutron star surface.

4.1. BL spectrum on the normal branch

Further along the Z-track of GX340+0, on normal and flaring branches, the fractional rms of the X-ray variability decreases significantly, by a factor of $\sim 5 - 10$. Nevertheless, the statistics is sufficient to place meaningful constrains on the first half of the normal branch. The data indicates that the behavior of the frequency resolved spectra does not change its character – at sufficiently high frequency, $f \gtrsim 1$ Hz, their shape does not depend upon the Fourier frequency and is significantly harder than the average spectrum and expected spectrum of the accretion disk. Therefore, we can conclude that frequency resolved spectra are representative of the spectrum of the boundary layer. Fit to the frequency resolved spectrum by Comptonization model requires infinitely large values of the Comptonization parameter. Correspondingly, it can be described by Wien or blackbody spectrum (they are close to each other $E \gtrsim 3$ keV range) with the best fit temperature of $kT \approx 2.4$ keV. The frequency resolved spectra (\approx boundary layer spectra) of GX340-0 on the normal and horizontal branch are compared in Fig. 6. Thus, with increase

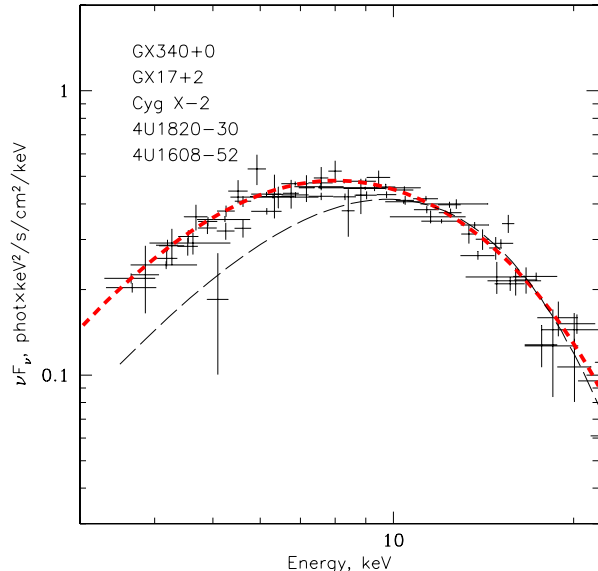


Fig. 5. Fourier-frequency resolved spectra (\approx boundary layer spectra) of 5 Z- and atoll sources (from Revnitsv & Gilfanov, 2005). For 4U1608-52 the frequency resolved spectrum of the lower kHz QPO is shown. All spectra were corrected for the interstellar absorption. The thick short-dashed line shows the best fit Comptonization model with $kT_s = 1.5$, $kT_e = 3.3$ keV, $\tau = 5$. The thin long-dashed line shows the blackbody spectrum with temperature $kT_{bb} = 2.4$ keV.

of the mass accretion rate up to a value close to critical Eddington rate the boundary layer spectrum in the 3–20 keV energy range approaches a Wien spectrum.

It would be interesting to follow up on these results and to consider the change of the BL spectrum from the horizontal to normal branch in other Z-sources. Unfortunately, in other four Z-sources from our sample the variability level on the normal branch is insufficient to obtain frequency resolved spectra with reasonable signal-to-noise ratio.

5. Nature of the Z-track

Knowledge of the shape of the boundary layer spectrum allows us to resolve the degeneracy caused by the similarity of the accretion disk and boundary layer spectra, which hindered many previous LMXB studies. As demonstrated by Gilfanov, Revnitsv & Molkov (2003), the spectra of atoll and Z-sources can be adequately described by the sum of the (renormalized) frequency resolved spectrum, representing the boundary layer component, and of the accretion disk emission (Fig. 4). The spectrum of the latter is well described by the general relativistic accretion disk model. The best fit values of the mass accretion rate are consistent with those inferred from the observed X-ray flux and accretion efficiency appropriate for a $1.4M_{\odot}$ neutron star with spin frequency of

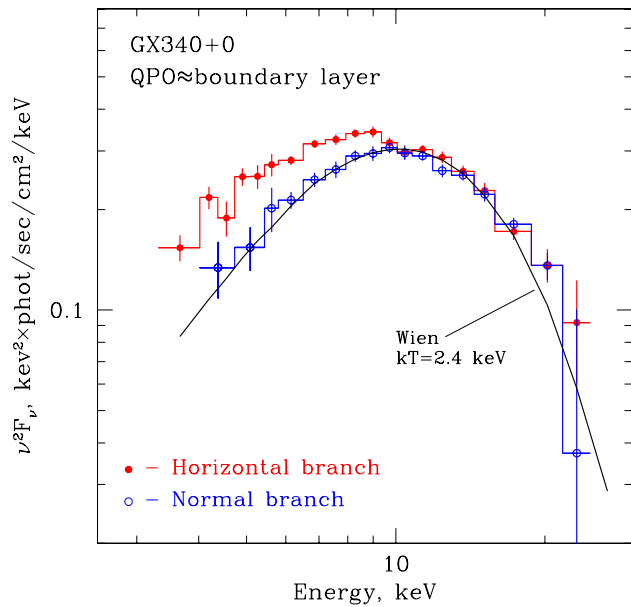


Fig. 6. The absorption corrected frequency resolved spectra of QPO (\approx boundary layer emission) in GX340 on the horizontal branch (lower \dot{M}) and upper half of the normal branch (higher \dot{M}). The horizontal branch data is same as in Fig. 1–4. The solid line shows Wien spectrum with $kT = 2.4$ keV.

~ 500 Hz. The agreement is especially remarkable, as the luminosity and mass accretion rate in atoll and Z-sources differ by the factor of ~ 10 .

We further exploit this approach and study the behavior of Z-sources in the color-color diagram in an attempt to relate the motion along the Z-track to changes of the physically meaningful parameters. We consider spectra integrated over 128-sec time intervals. As above, these spectra are fitted with a model, consisting of the boundary layer and the accretion disk components. The shape of the boundary layer spectrum was approximated by the *comptt* model with parameters from the section 4. For the accretion disk spectrum we adopt the multicolor disk model (*diskbb* model in XSPEC) or general relativistic accretion disk model (*grad*). The model adequately describes observed spectra on the normal and horizontal branch. Further details of the analysis method, limitations of the model and discussion of results are presented in Revnivtsev & Gilfanov (2005).

5.1. BL fraction

The dependences of the BL contribution to the total X-ray emission on the position on the Z-track are plotted in Fig. 7. The coordinate along the Z-track was defined to be proportional to the hard color with the reference points $S_Z = 1, 2$ corresponding to the turning points of the “Z”, as is commonly used for such plots. Statistical uncertainties in the values of the BL fraction are small and can be neglected, as confirmed by the dispersion of the points in Fig. 7. More important are the systematic ones associated with the im-

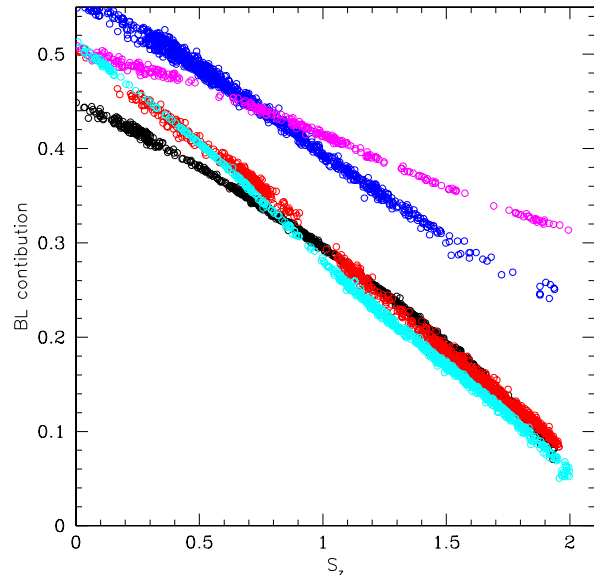


Fig. 7. Dependence of the boundary layer contribution to the total X-ray emission of Z-sources as a function of the position on the Z-diagram

precise knowledge of the shape of the BL spectrum and its possible variations along the Z-track. As demonstrated in Revnivtsev & Gilfanov (2005) their amplitude does not exceed $\sim 0.05 - 0.1$ in the units of Fig. 7.

The Fig. 7 suggests that the boundary layer fraction decreases along the Z-track and it is smaller on the normal branch than on the horizontal branch. As discussed in Revnivtsev & Gilfanov (2005), this conclusion is rather robust, as long as the assumption regarding the constancy of the boundary layer spectrum is approximately correct. As the variability at $f \gtrsim 1$ Hz is primarily associated with the boundary layer emission, the decrease of the boundary layer fraction along the Z-track also explains well-known decrease of the level of aperiodic and quasi-periodic variability.

Although no simple physical interpretation of the observed behavior can be offered, we mention several possibilities. One of these is that the general structure of the accretion flow does not change significantly and $\sim 50\%$ of the energy is always released on, or very close to the neutron star surface. The apparent decrease of the boundary layer fraction on the normal branch is a result of its geometrical obscuration by, for example, the geometrically thickened accretion disk. An alternative possibility is that at high values of the mass accretion rate $\dot{M} \sim \dot{M}_{\text{Edd}}$ a significant modification of the accretion flow structure occurs and its division into two geometrically distinct parts – boundary layer and accretion disk, becomes inapplicable. Namely, due to non-negligible pressure effects the deceleration of the orbital motion of the accreting matter from Keplerian frequency to the neutron star spin frequency would take place in a geometrically extended region with the radial extend of $\Delta R \sim R_{\text{NS}}$. In this case, the

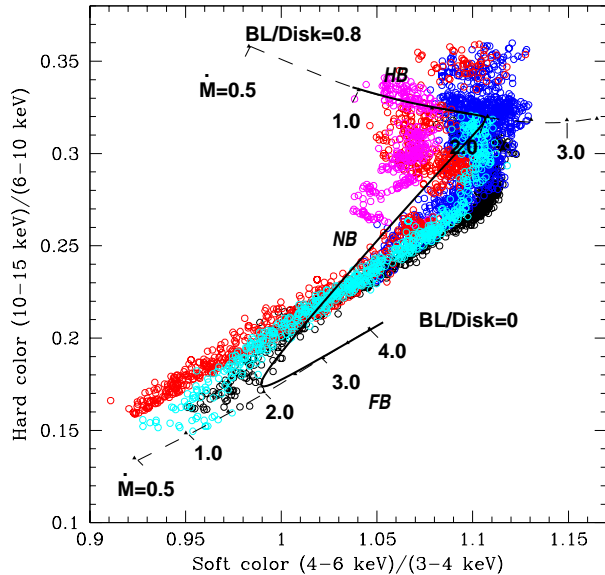


Fig. 8. The horizontal and normal branches in the color-color diagram of several Z-sources (Cyg X-2, GX340+0, Sco X-1, GX 5-1 and GX 17+2). Overlaid on the data are the tracks predicted by the model (section 5.2). The two thick dashed lines show evolution of the colors with change of the accretion rate in the disk for two different values of the BL fraction: 44% (upper) and zero (lower). The values of the mass accretion rates \dot{M} of the disk component are marked in units of 10^{18} g/s. The thick solid line shows the Z track with transition at $\dot{M} \sim 2 \cdot 10^{18}$ g/s.

observed decrease of the boundary layer fraction could reflect actual decrease of the fraction of the energy released on the neutron star surface with the rest of the energy being released in the extended transition region.

5.2. Shape of Z-diagram

Motivated by these results we use the two-component spectral model to explain the shape of the Z-track on the color-color diagram. For this purpose, the accretion disk component is modeled by the general relativistic accretion disk model of Ebisawa et al. (1991) (the *grad* model in XSPEC) which explicitly includes dependence on the mass accretion rate. Using this spectral model we can calculate the position in the color-color diagram as a function of the mass accretion rate and the boundary layer fraction. This is an attempt to understand general tendencies of the Z-diagram, rather than to construct its precise quantitative description.

The results are presented in Fig. 8. The two dashed curves in the figure show the evolution of spectral colors with the increase of \dot{M} for two values of the boundary layer fraction, BL/disk=0.8 and BL fraction of zero. The evolution of colors corresponding to a change of the BL contribution from

$F_{\text{BL}}/F_{\text{disk}} = 0.8$ to zero at $\dot{M} \sim 2 \times 10^{18}$ g/s is shown by the thick solid line.

The general shape of the Z-track can be reproduced in the model as a result of variation of two parameters – the mass accretion rate and BL fraction. The mass accretion rate increases along the Z-track. The Z-shape of the track is defined by the variation of the BL fraction, which decreases along the “standard” theories to a small number of the order of \sim zero at the end of the normal branch. The exact value of \dot{M} , corresponding to the transition from the horizontal to the normal branch depends on the disk model parameters – the binary system inclination, the mass of the neutron star and the spectral hardening factor. For our choice of parameters, it equals $\dot{M} \sim 2 \cdot 10^{18}$ g/sec, i.e. is of the order of the Eddington critical value for a $1.4M_{\odot}$ neutron star.

6. Summary

1. The X-ray variability in luminous LMXBs on the short timescales, $f \gtrsim 1$ Hz, is caused by variations of the luminosity of the boundary layer. The accretion disk emission is significantly less variable at these frequencies. The BL spectrum remains nearly constant in the course of luminosity variations and its shape equals the frequency resolved spectrum, i.e. can be directly derived from the timing data (Fig. 4).
2. In the investigated range of the mass accretion rate $\dot{M} \sim (0.1 - 1)\dot{M}_{\text{Edd}}$, the boundary layer spectrum depends weakly on \dot{M} . Its shape is remarkably similar in atoll and Z-sources (Fig. 5), despite an order of magnitude difference in the mass accretion rate. Data indicates that in the limit of high $\dot{M} \sim \dot{M}_{\text{Edd}}$, the boundary layer spectrum can be described by Wien spectrum with $kT \approx 2.4$ keV (Fig. 6). At lower values of \dot{M} the spectra are better described by model of saturated Comptonization with electron temperature of $\sim 2 - 4$ keV and Comptonization parameter $y \sim 1$. Weak dependence of the BL spectrum on the global value of \dot{M} lends support to the theoretical suggestion by Inogamov & Sunyaev (1999) that the boundary layer is radiation pressure supported.
3. The kHz QPOs appear to have the same origin as aperiodic and quasiperiodic variability at lower frequencies. The msec flux modulations originate on the surface of the neutron star although the kHz “clock” might reside in the disk or be determined by the disk – neutron star interaction.
4. We attempt to relate the motion of Z-sources along the Z-track to changes in the values of the physically meaningful parameters. Our results suggest that the contribution of the boundary layer component to the observed emission decreases along the Z-track from the conventional value of $\sim 50\%$ on the horizontal branch to a rather small number at the end of the normal branch (Fig. 7, 8). The main difference of our approach from previous attempts is in the a priori knowledge of the shape of the boundary layer spectrum. This allowed us to avoid ambiguity of

the spectral decomposition into boundary layer and disk components.

Acknowledgements. This research has made use of data obtained through the High Energy Astrophysics Science Archive Research Center Online Service, provided by the NASA/Goddard Space Flight Center.

References

- Barret D., 2001, *AdSpR*, 28, 307
- Bradt, H., Rotshild, R., Swank, J. 1993, *Astron. Astrophys. Suppl. Ser.* 97, 355
- Dieter, S., Vaughan, B., Kuulkers, E. et al. 2000, *A&A*, 353, 203
- Di Salvo, T., Robba, N., Iaria, R. et al. 2001, *ApJ*, 554, 49
- Done, C., Zyccki, P. T. & Smith, D. A. 2002, *MNRAS*, 331, 453
- Ebisawa, K., Mitsuda, K. & Hanawa, T. 1991, *ApJ*, 367, 213
- Gierlinski, M., Zdziarski, A.A., Done, C. et al. 1997, *MNRAS*, 288, 958
- Gilfanov, M., Churazov, E., Revnivtsev, M. 2000, *MNRAS*, 316, 923
- Gilfanov, M., Revnivtsev, M., & Molkov, S. 2003, *A&A*, 410, 217
- Grebenev, S. & Sunyaev, R. 2002, *Astronomy Letters*, 28, 150
- Inogamov, N. & Sunyaev, R. 1999, *Astr.Lett*, 25, 269
- Kluzniak, W. 1988, PhD Thesis
- Kuulkers E., van der Klis M., Oosterbroek T., Asai K., Dotani T., van Paradijs J., Lewin W. H. G., 1994, *A&A*, 289, 795
- Mendez, M., van der Klis, M., van Paradijs, J. et al. 1997, *ApJ*, 485, 37
- Mitsuda, K., Inoue, H., Koyama, K. et al. 1984, *PASJ*, 36, 741
- Mitsuda, K. & Tanaka, Y., In: *The evolution of galactic X-ray binaries; Proceedings of the NATO Advanced Research Workshop, Rottach-Egern*, D. Reidel Publishing Co., 1986, p. 195.
- Popham, R. & Sunyaev, R. 2001, *ApJ*, 547, 355
- Revnivtsev, M., Gilfanov, M. & Churazov, E. 1999, *A&A*, 347, 23
- Revnivtsev, M. & Gilfanov, M. 2005, *A&A*, submitted (astro-ph/0506019)
- Ross, R. & Fabian, A. 1996, *MNRAS*, 281, 637
- Shakura, N.I. & Sunyaev, R.A. 1973, *A&A*, 24, 337
- Shakura, N.I. & Sunyaev, R.A. 1988, *Ad.Sp.R.*, 8, 135
- Shimura, T. & Takahara, F. 1995, *ApJ*, 331, 780
- Sibgatullin, N. & Sunyaev, R. 2000, *Astr.Lett.*, 26, 699
- Sunyaev, R. & Shakura, N. 1986, *SvAL*, 12, 117
- van der Klis, M. 1986, *Lecture Notes in Physics*, 266, 157
- van der Klis, M. 2000, *ARA&A*, 38, 717
- Vaughan, B., van der Klis, M., Lewin, W. et al. 1994, *ApJ*, 421, 738
- Vaughan, B., van der Klis, M., Lewin, W. et al. 1999, *A&A*, 343, 197
- White, N., Stella, L., Parmar, A. 1988, *ApJ*, 324, 363